Journal of Molecular Catalysis A: Chemical 338 (2011) 51–57

Contents lists available at ScienceDirect

Journal of Molecular Catalysis A: Chemical

journal homepage: www.elsevier.com/locate/molcata

Bio-relevant manganese(II) compartmental ligand complexes: Syntheses, crystal structures and studies of catalytic activities

Averi Guha[a], Kazi Sabnam Banu[a], Arpita Banerjee[a], Totan Ghosh[a], Santanu Bhattacharya[b], Ennio Zangrando[c,*], Debasis Das[a,*]

[a] Department of Chemistry, University of Calcutta, 92, A.P.C. Road, Kolkata 700009, India
[b] Department of Chemistry, Maharaja Manindra Chandra College, Kolkata 700003, India
[c] Dipartimento di Scienze Chimiche e Farmaceutiche, University of Trieste, Via L. Giorgieri 1, 34127 Trieste, Italy

ARTICLE INFO

Article history:
Received 22 September 2010
Received in revised form 23 January 2011
Accepted 24 January 2011
Available online 24 February 2011

Keywords:
Manganese(II)
Schiff-base complexes
Catecholase activity
Phosphatase activity
Crystal structure

ABSTRACT

Three new mono-manganese(II) complexes of a compartmental ligand, namely $[Mn(HL)(H_2O)_3](NO_3)_2{\cdot}H_2O$ (**1**), $[Mn(HL)(SCN)_2(H_2O)]{\cdot}H_2O$ (**2**), and $[Mn(HL)\{N(CN)_2\}(H_2O)_2](NO_3){\cdot}H_2O$ (**3**), where L = 2,6-bis{2-(N-ethyl)pyridineiminomethyl}-4-methylphenolato, have been synthesized and characterised by routine physicochemical techniques and complexes **1**, **2** also by X-ray single crystal structure analysis. All the mono nuclear complexes contain Mn^{II} high spin species at octahedral core as evidenced by magnetic moment (measured at 300 K) and EPR study at 77 K. As revealed by crystal structure analyses, the protonation of one imine nitrogen atom of the potential dinucleating ligand L hampers to form the expected dinuclear Mn^{II} complex. However, complexes **1**–**3** show excellent catecholase-like activity with both 3,5-di-*tert*-butylcatechol and tetrachlorocatechol as substrates. In addition complexes **1** and **2** also exhibit phosphatase activity, while **3** forms an adduct with *p*-nitrophenyl phosphate as substrate. To the best of our knowledge this is the first report of Mn^{II} complexes being able to catalyze the oxidation of TCC to TCQ. Catecholase and phosphatase activities have been monitored by UV–vis spectrophotometer and Michaelis–Menten equation has been applied to rationalize all the kinetic parameters where complex **1** shows maximum k_{cat} value followed by **2** and **3** (where for phosphatase activity **3** only forms an adduct).

1. Introduction

Phenol based compartmental ligands are of current interest to the bio-inorganic chemists as the most desirable target to synthesize dinuclear complexes as corroborative models of some metallobiosites namely catechol oxidase, urease, catalase etc. [1–12]. Recently our group have got excellent results while working with phenol based compartmental ligand complexes of Ni^{II}, Cu^{II} and Zn^{II} [13]. Manganese is one of the most important trace transition element in biological systems, being present in several metalloenzymes of varied nuclearity. Literature survey reveals that although manganese is one of the most important trace transition element in biological systems (being present in several metalloenzymes with varying nuclearity, e.g. mononuclear manganese species exist in superoxide dismutase [14] and manganese dioxygenase [15], as dinuclear species in catalase [16,17], ribonucleotide reductase [18], and arginase [19] and as the tetra nuclear cluster found in the oxygen evolving complex (OEC) of photo system II (PS II) [20–24]) the reports on bio-relevant catalytic activities of manganese(II) compartmental ligand complexes are surprisingly scanty.

We started this work with the goal to generate manganese mimics of catecholase [dicopper(II) containing type-III copper protein] and of phosphatase [dizinc(II) containing hydrolase enzyme] since such reports are rare in literature. In order to stabilize manganese in its +2 oxidation state, we have accordingly designed a phenol based compartmental ligand, 2,6-bis{2-(N-ethyl)pyridineiminomethyl}-4-methylphenolato (L) as depicted in Scheme 1, a system having vacant π^* orbitals, necessary condition to stabilize metals in low oxidation states. Interestingly, instead of getting dinuclear manganese(II) complexes we have obtained mono-manganese(II) species, $[Mn(HL)(H_2O)_3](NO_3)_2{\cdot}(H_2O)$ (**1**), $[Mn(HL)(SCN)_2(H_2O)]{\cdot}0.5H_2O$ (**2**) and $[Mn(HL)\{N(CN)_2\}(H_2O)_2](NO_3){\cdot}H_2O$ (**3**) most likely due to the protonation of one of the imine nitrogen atoms of the dinucleating ligand, L. As a result of such peculiarities of the structures these three complexes show excellent catalytic activities. Here

* Corresponding authors. Tel.: +91 33 24837031; fax: +91 33 23519755.
E-mail address: dasdebasis2001@yahoo.com (D. Das).

1381-1169/$ – see front matter © 2011 Elsevier B.V. All rights reserved.
doi:10.1016/j.molcata.2011.01.025

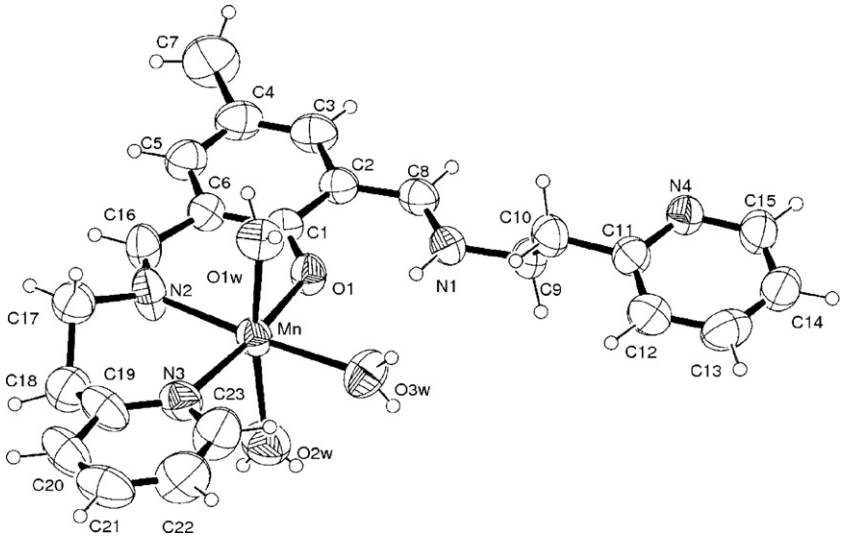

Fig. 1. ORTEP drawing (30% probability ellipsoid) of the complex cation of **1**. Of the disordered ethylene bridge only the C17/C18 atoms at higher occupancy are shown.

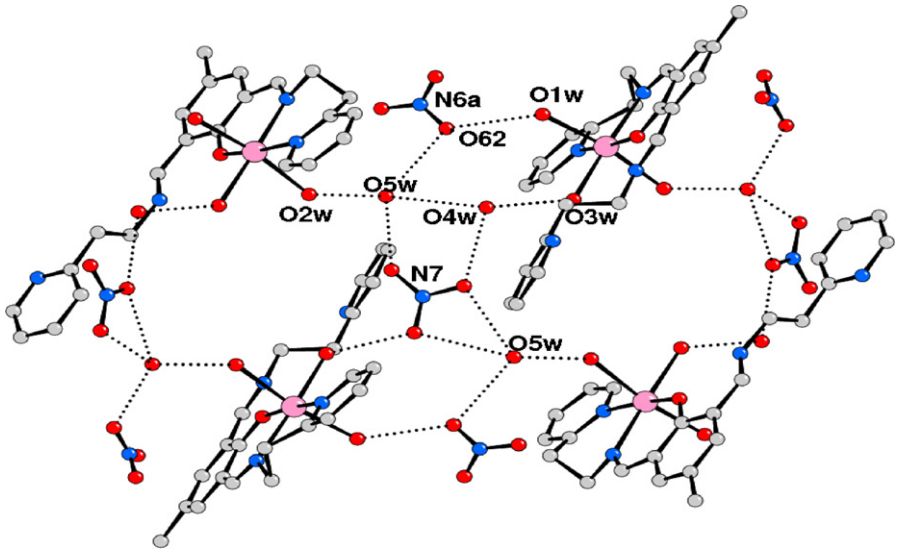

Fig. 2. Detail of the H-bonding pattern in the crystal packing of **1**. Ow4 and nitrate N7 are close to a centre of symmetry and their positions can be interchanged.

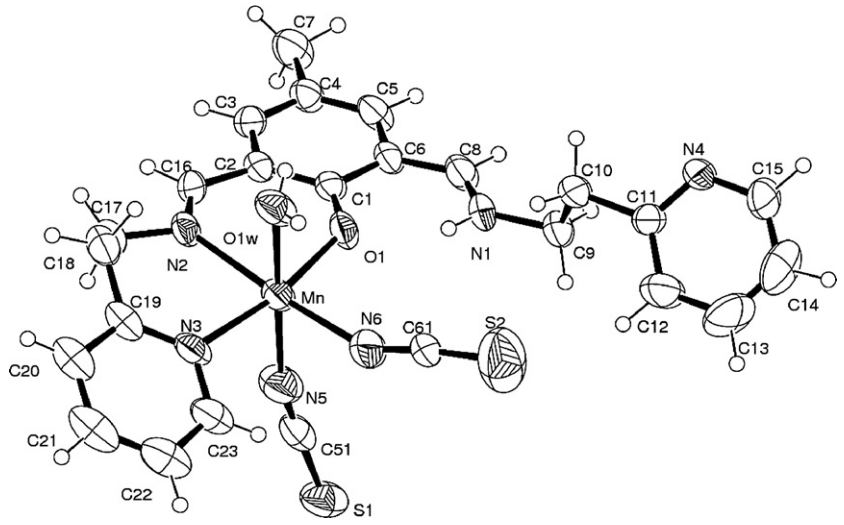

Fig. 3. ORTEP drawing (40% probability ellipsoid) of complex **2**.

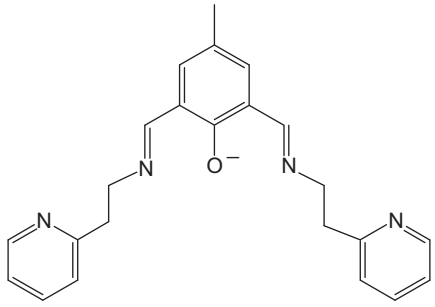

Scheme 1. Chemical structure of compartmental ligand L.

we are reporting their synthetic technique, characterisation, and catalytic activities.

2. Results and discussion

2.1. Syntheses and characterisation

Complex **1** is prepared by applying template synthesis technique by treating manganese(II) nitrate hydrate with the Schiff-base formed *in situ* via condensation of 2,6-diformyl-4-methylphenol with 2-(2-aminoethyl)pyridine in methanol. Complexes **2** and **3** are obtained by adding an excess of sodium thiocyanate and sodium dicyanamide (at least twice with respect to the manganese (II) nitrate salt) to the solution of **1**, respectively.

Complexes **1**–**3** show bands in IR spectra in the range 1642–1645 cm^{-1} and 1532–1540 cm^{-1} due to C=N stretching and skeletal vibration, respectively. The bands in the range 1320–1383 cm^{-1} observed in the IR spectra of complexes **1** and **3** are due to NO_3^- group [25]. Complex **2** shows a band centred at 2165 cm^{-1} corresponds to the SCN^- moiety. The very strong absorptions in the region of 2140–2160 cm^{-1} observed in the IR spectrum of complex **3** is due to ν(C≡N) of $N(CN)_2^-$ moiety present in it. The effective magnetic moment for complexes **1**–**3** in the range of 5.85–5.90 B.M. at 300 K is very much consistence with the spin only value (5.92 B.M.) for high spin Mn^{II}. The oxidation state of the metal complexes has further been examined by EPR study at liquid nitrogen temperature (77 K) in methanol. All the complexes **1**–**3** exhibit characteristics six line EPR spectra (in SI file) as it is expected for octahedral Mn^{II} species.

2.2. Description of structure of complexes *1* and *2*

Complex **1** shows the manganese ion in a distorted octahedral geometry being chelated in the equatorial plane by the compartmental ligand through the phenolato oxygen, the imino and the pyridine nitrogen donors and completing the coordination sphere with three water molecules. A picture of the complex is depicted in Fig. 1, and a selection of bond lengths and angles is reported in Table 1.

The geometrical values are as expected, with Mn–N(py) and Mn–O2w that manifest the longest values of 2.264(3) and 2.238(4) Å, respectively. The other coordination bond lengths fall in range 2.102(2)–2.195(3) Å. The distortions in the coordination bond angles are evident from Table 1, the larger from ideal value being O(1w)–Mn–O(2w) of 170.10(14)°. The protonated imino nitrogen N1 forms an intramolecular H-bond with the phenolato oxygen O1 (N···O distance 2.580 Å), and the molecules are arranged in pairs about a centre of symmetry connected by a strong O1w–H···N4(pyridine) hydrogen bond (N4···O1w = 2.580 Å), an arrangement similar to that observed in **2** (see below). Moreover the coordinated and lattice water molecules are engaged in a H-bonding scheme with the nitrate anions leading to a 3D polymeric

Table 1
Selected bond lengths (Å) and angles (°) for **1** and **2** with esds in parentheses.

	1		2
Mn–O(1)	2.102(2)	Mn–O(1)	2.142(4)
Mn–N(2)	2.195(3)	Mn–N(2)	2.219(5)
Mn–N(3)	2.264(3)	Mn–N(3)	2.319(6)
Mn–O(1w)	2.190(3)	Mn–O(1w)	2.278(6)
Mn–O(2w)	2.238(4)	Mn–N(5)	2.231(7)
Mn–O(3w)	2.180(3)	Mn–N(6)	2.139(7)
O(1)–Mn–N(2)	83.45(9)	O(1)–Mn–N(2)	82.60(18)
O(1)–Mn–N(3)	172.55(10)	O(1)–Mn–N(3)	170.5(2)
O(1)–Mn–O(1w)	91.03(9)	O(1)–Mn–O(1w)	94.75(19)
N(2)–Mn–N(3)	89.15(11)	N(2)–Mn–N(3)	88.9(2)
N(2)–Mn–O(1w)	92.34(14)	N(2)–Mn–O(1w)	84.27(19)
N(3)–Mn–O(1w)	90.06(10)	O(1w)–Mn–N(3)	80.2(2)
N(2)–Mn–O(2w)	97.56(17)	N(2)–Mn–N(5)	97.8(2)
N(2)–Mn–O(3w)	173.02(12)	N(2)–Mn–N(6)	173.5(3)
N(3)–Mn–O(2w)	89.96(12)	N(3)–Mn–N(5)	97.9(2)
N(3)–Mn–O(3w)	97.77(12)	N(3)–Mn–N(6)	90.6(3)
O(1)–Mn–O(2w)	90.23(12)	O(1)–Mn–N(5)	87.5(2)
O(1)–Mn–O(3w)	89.62(10)	O(1)–Mn–N(6)	97.4(3)
O(1w)–Mn–O(2w)	170.10(14)	O(1w)–Mn–N(5)	177.1(2)
O(1w)–Mn–O(3w)	88.58(12)	O(1w)–Mn–N(6)	89.3(3)
O(2w)–Mn–O(3w)	81.61(15)	N(5)–Mn–N(6)	88.7(3)

arrangement (Fig. 2). However, being the nitrate and the water molecules disordered as described in Section 3, this aspect will not be described in details. A π–π interaction is realized between the uncoordinated py and the phenolato ring of an adjacent complex (distance between ring centroids 3.675 Å, angle 6.7°).

The molecular structure of complex **2** is similar to that of **1** by replacing two aqua ligands in the axial and equatorial positions by SCN^- anions coordinated via N. The coordination bond lengths appear systematically slightly longer than the corresponding ones of complex **1**. A picture of the complex is depicted in Fig. 3, and a selection of bond lengths and angles is reported in Table 1. The equatorial Mn–N(6) CS distance (2.139(7) Å) is shorter than the axial Mn–N(5) CS of 2.231(7) Å, and the relative C–N–Mn angles are 146.3(7) and 166.5(6)°. The larger value for the latter can be explained with the requirement of sulphur S1 to establish a S1···H–O1w (at −1 + *x*, *y*, *z*) interaction with an adjacent molecule (S···O distance 3.219 Å). The intramolecular N1–H···O1 interaction has a distance of 2.564 Å. The molecules are arranged in pairs about a centre of symmetry connected by a strong O1w–H···N4(pyridine) hydrogen bond (N···O distance = 2.720 Å), as shown in Fig. 4.

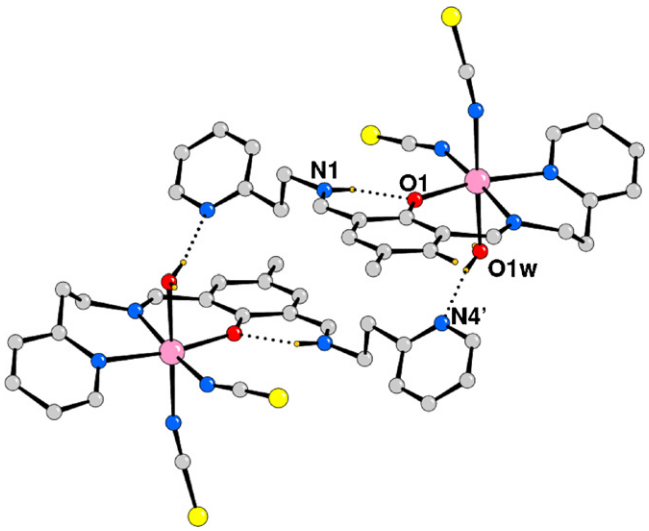

Fig. 4. H-bonded centrosymmetric arrangement of complex **2**.

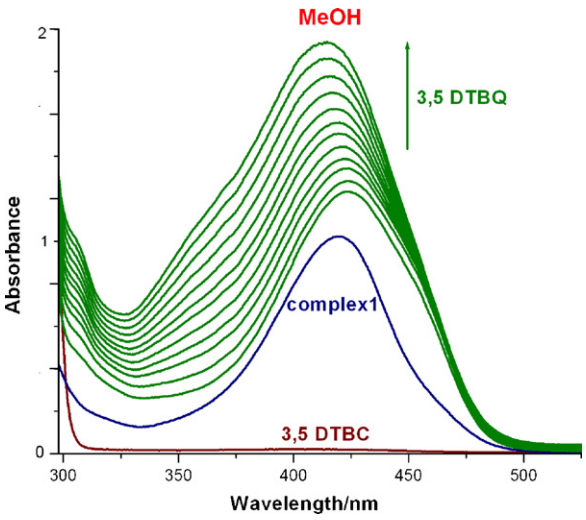

Fig. 5. UV–vis spectra of (i) complex **1** (1×10^{-4} M) in methanol; (ii) 3,5-DTBC (1×10^{-2} M) in methanol; (iii) changes in UV–vis spectra of **1** upon addition of 100-fold 3,5-DTBC observed at intervals of 10 min.

Any attempt to obtain suitable single crystals for X-ray analysis of complex **3** failed. However preliminary results from a disordered crystal allowed to confirm the formation of a mononuclear manganese complex, namely $[Mn(HL)(H_2O)_3](N(CN)_2)(NO_3)$, a composition confirmed by routine physicochemical techniques (*vide supra*). Since the coordination ability of $N(CN)_2^-$ is well documented, we cannot rule out that in solution this anion might be in the first coordination sphere of the metal, and thus committed in the catalytic activity of this complex (see below).

2.3. Catalytic activity and kinetic study

2.3.1. Catecholase activity

The enzymes catechol oxidases [26,27], found in bacteria, fungi and plants, belong to the class of type-III copper enzyme [28] like hemocyanin and tyrosinase and are also known as *o*-diphenol oxidases or polyphenol oxidases. Catechol oxidases catalyze exclusively the two-electron oxidation of *o*-diphenols (*i.e.* catechols) to the corresponding *o*-quinones (called catecholase activity) coupled with the reduction of dioxygen to water. The resulting highly reactive quinones auto polymerize to form brown polyphenolic catechol melanins. Some higher valent manganese complexes are observed to exhibit this property [29,30]. We have examined the catalytic activity of complexes **1**–**3** evaluating the oxidation of 3,5-di-*tert*-butylcatechol (3,5-DTBC) and tetrachlorocatechol (TCC) by O_2 to *o*-quinone (3,5-DTBQ and TCQ, respectively) in air-saturated methanol solution at 300 K. All the three mononuclear Mn^{II} complexes show significant catalytic oxidation of both the substrates as monitored by means of UV–vis spectroscopy. The kinetics for the oxidation of the substrates 3,5-DTBC and TCC were determined by monitoring the increase of the products, 3,5-DTBQ and TCQ, respectively, following the procedure reported in Section 3. All the species exhibit saturation kinetics and complex **1**, with three labile water molecules bound to the metal centre, shows the highest k_{cat} value and **3** the lowest among the three complexes. The UV–vis spectral scan and enzyme kinetics data of complex **1** with 3,5-DTBC and TCC are depicted in Figs. 5–8, the corresponding spectral scans and enzyme kinetics data for complexes **2** and **3** are reported as SI file.

2.3.2. Phosphatase activity

Phosphatase or phosphohydrolase enzymes exclusively catalyze the hydrolytic cleavage of P–O linkage of phosphate esters (phosphatase activity) [31–33]. It is well-known that phosphate

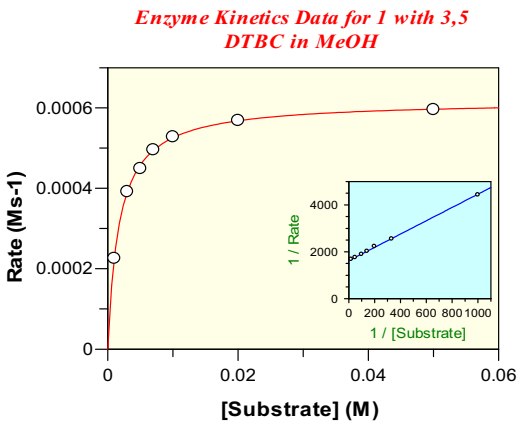

Parameter	Value	Std. Error
Vmax	0.0006	3.31185e-006
Km	0.0018	4.39600e-005

Fig. 6. Plot of rate vs concentration of **1**. Plot of inset shows reciprocal Lineweaver–Burk plot for the same complex.

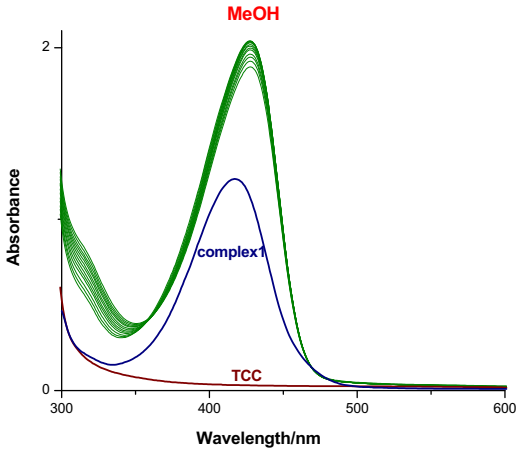

Fig. 7. UV–vis spectra of (i) complex **1** (1×10^{-4} M) in methanol; (ii) TCC (1×10^{-2} M) in methanol; (iii) changes in UV–vis spectra of **1** upon addition of 100-fold TCC observed at intervals of 10 min.

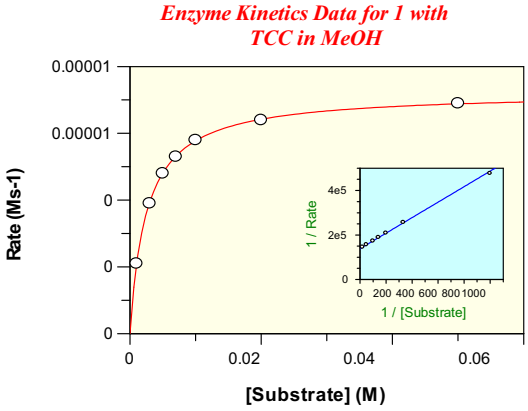

Parameter	Value	Std. Error
Vmax	7.22828e-006	2.70873e-008
Km	0.0025	3.79520e-005

Fig. 8. Plot of rate vs concentration of **1**. Plot of inset shows reciprocal Lineweaver–Burk plot for the same complex.

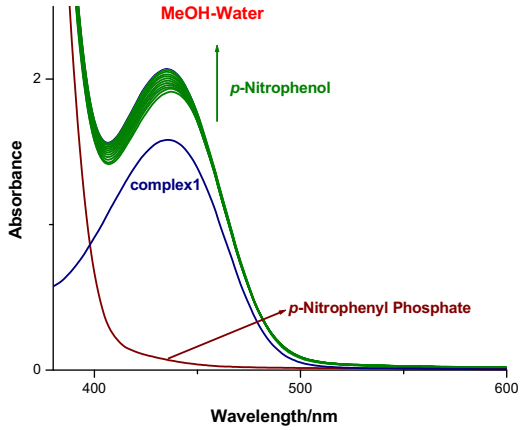

Fig. 9. UV–vis spectra of (i) complex **1** (1×10^{-4} M) in methanol–water; (ii) PNPP (1×10^{-2} M) in methanol–water; (iii) changes in UV–vis spectra of **1** upon addition of 100-fold PNPP observed at intervals of 10 min.

ester backbone is usually highly resistant towards hydrolytic cleavage and therefore it is still a big challenge to synthesize catalysts reactive enough to hydrolyze the target bonds rapidly under physiological conditions. Complexes **1** and **2** are potential catalysts to cleave the P–O linkage due to their structural property. The activity was monitored by UV–vis spectroscopy using PNPP as substrate in MeOH–water medium and kinetic parameters were evaluated on the basis of initial rate method at 300 K using the Michaelis–Menten equation where a saturation kinetics were attained after a short period of time. The kinetic study was performed following the procedure reported by Chattopadhyay et al. [13a]. In this case also complex **1** shows a greater k_{cat} value than that of complex **2** and complex **3** forms an adduct with PNPP. The UV–vis spectral scan and enzyme kinetics data of complex **1** with PNPP are shown in Figs. 9 and 10, while the corresponding spectral scans and enzyme kinetics data of **2** and **3** are given in SI file.

A blank experiment, carried out with only Mn^{2+} salt and the substrates in the absence of the ligand, showed no band around ~400 nm in the UV–vis spectra, as illustrated in Fig. 11 with 3,5-DTBC as substrate (results for TCC and PNPP as substrates are

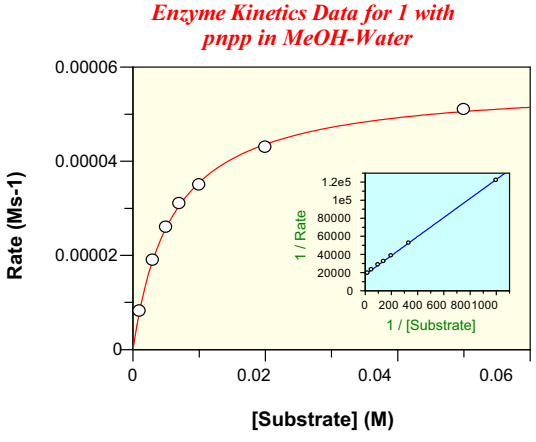

Parameter	Value	Std. Error
Vmax	5.65636e-005	5.51194e-007
Km	0.0060	0.0002

Fig. 10. Plot of rate vs concentration of **1**. Plot of inset shows reciprocal Lineweaver–Burk plot for the same complex.

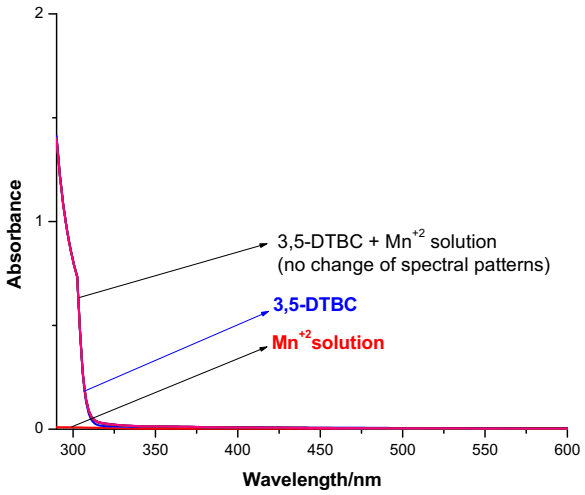

Fig. 11. UV–vis spectrum of (i) Mn^{2+} salt solution (1×10^{-4} M) in methanol; (ii) 3,5-DTBC (1×10^{-2} M) in methanol; (iii) UV–vis spectra of Mn^{2+} salt solution upon addition of 100-fold 3,5-DTBC observed at intervals of 10 min.

reported as SI) suggesting the effectiveness of our complexes as catalyst.

2.3.3. *Rationalization of the observed k_{cat} values*

The catalytic activities exhibited by these low valent Mn-complexes depend mainly on the ease of interaction between the substrate and the catalyst. More facile interaction would lead to greater k_{cat} value. Again the feasibility of the interaction depends on the structure of the catalyst where unsaturation of the coordination site or presence of labile groups attached to the metal centre in the coordination sphere promotes the approach of the substrate to a greater extent. Complex **1** has three labile water molecules in its coordination sphere and thus the approach of substrates towards the metal centre should be easier in comparison to the other two complexes, where one and two water molecules are present in **2** and in **3**, respectively, leading complex **1** to display the highest k_{cat} value (Table 2). The bulkier dicyanamide present in **3** (with regard to thiocyanate in **2**) could justify a more facile interaction of the substrate to the metal centre in **2**, thus validating the observed higher k_{cat} value of **2** than of **3** in case of catecholase activity, while only an adduct is formed between **3** and PNPP in the phosphatase activity study. However, electronic effects of dicyanamide moiety and thiocyanate anions cannot be excluded to influence these reactions. Although the formal oxidation state of manganese in our complexes is +2, the catalytic activity exhibited by them is largely due to the presence of positive charge (on imine N) very near to the metal centre. This extra positive charge can furnish a path to facilitate the approach of the negatively charged substrate to bind the metal centre, a well accepted argument nowadays in biology/bioinorganic chemistry to explain the activity of metallobiosites such as CuZn–SOD [34–37].

Table 2
k_{cat} values (h^{-1}) of complexes **1**, **2** and **3** catalyzed reactions with 3,5-DTBC, TCC and PNPP as substrates.

Complex	3,5-DTBC	TCC	PNPP
1	2.16×10^4	2.60×10^2	2.03×10^3
2	1.44×10^4	2.46×10^2	1.23×10^3
3	7.2×10^3	2.16×10^2	Adduct

Table 3
Crystal data and details of structural refinements for **1** and **2**.

	1	**2**
Empirical formula	$C_{23}H_{32}MnN_6O_{11}$	$C_{25}H_{26}MnN_6O_2S_2$
fw	623.49	561.58
Cryst syst	Monoclinic	Monoclinic
Space group	$C\,2/c$	$P\,2_1/c$
a (Å)	17.571(4)	9.2223(10)
b (Å)	17.069(3)	19.601(2)
c (Å)	20.509(4)	14.6243(16)
β (°)	109.87(3)	94.664(2)
V (Å^3)	5785(2)	2634.8(5)
Z	8	4
D_{calcd} (mg/m^3)	1.432	1.416
M (Mo Kα) (mm^{-1})	0.523	0.694
F(0 0 0)	2600	1164
θ range (°)	3.56–26.02	1.74–23.24
Collected reflections	38868	13890
Indep reflections	5629	3153
R_{int}	0.0380	0.0516
Obs reflections [$I > 2\sigma(I)$]	3426	2307
Parameters	434	333
R_1 [$I > 2\sigma(I)$]	0.0576	0.0623
wR_2 [$I > 2\sigma(I)$]	0.1712	0.1672
GOF on F^2	1.036	1.081
Residuals/e Å^{-3}	0.380, −0.318	0.876, −0.598

3. Experimental

3.1. Starting materials

All chemicals were obtained from commercial sources and used as received. Solvents were dried according to standard procedure and distilled prior to use. 2,6-Diformyl-4-methylphenol was prepared according to the literature method [38]. 2-(2-Aminoethyl) pyridine (Lancaster Chemical Company Inc.), manganese(II) nitrate hydrate (Aldrich), sodium thiocyanate (SRL Pvt. Ltd.), sodium dicyanamide (Fluka) were purchased from commercial sources and used as received. All other chemicals used were of AR grade.

3.2. Physical measurements

Elemental analyses (carbon, hydrogen, and nitrogen) were performed using a PerkinElmer 240C elemental analyzer. Infrared spectra (4000–400 cm^{-1}) were recorded at 300 K using a Shimadzu FTIR-8400S with KBr as medium. Electronic spectra (800–200 nm) were obtained at 300 K using a Shimadzu UV-3101PC with dry methanol as medium as well as reference. EPR experiment was done at 298 K and 77 K in pure methanol using Bruker EMX-X band spectrometer. The magnetic susceptibilities were measured at 300 K using a Magway MSB Mk 1 magnetic susceptibility balance made by Sherwood Scientific Ltd.

3.3. Syntheses of the complexes

3.3.1. Complex **1**: $[Mn(HL)(H_2O)_3](NO_3)_2{\cdot}H_2O$

A methanolic solution (5 mL) of 2-(2-aminoethyl)pyridine (0.244 g, 2 mmol) was added dropwise to a heated methanolic solution (10 mL) of 2,6-diformyl-4-methylphenol (0.164 g, 1 mmol), and the resulting orange colour solution was boiled for half an hour. Then, a methanolic solution (15 mL) of $Mn(NO_3)_2{\cdot}3H_2O$ (0.7176 g, 2.5 mmol) was added and reflux was further continued for 2 h. After cooling, the clear orange solution was kept in a $CaCl_2$ desiccator in dark. Square-shaped orange crystals, suitable for X-ray data collection were obtained after a few days from that solution (yield 68%). Anal. Calcd. for $C_{23}H_{32}N_6O_{11}Mn$ (**1**): C, 44.31; H, 5.17; N, 13.48. Found: C, 44.12; H, 5.26; N, 13.38%.

3.3.2. Complex **2**: $[Mn(HL)(SCN)_2(H_2O)]{\cdot}H_2O$

The complex was prepared following the same procedure as for **1** with the addition of solid NaSCN (0.3242 g, 5 mmol) on the resulting cooled mixture and stirred for 3 h. The clear orange solution was kept in a $CaCl_2$ desiccator in dark, from which square-shaped orange crystals, suitable for X-ray data collection, were obtained after a few days (yield 70%). Anal. Calcd. for $C_{25}H_{27}N_6O_{2.5}S_2Mn$ (**2**): C, 52.63; H, 4.77; N, 14.73. Found: C, 52.59; H, 4.66; N, 14.62%.

3.3.3. Complex **3**: $[Mn(HL)\{N(CN)_2\}(H_2O)_2](NO_3){\cdot}H_2O$

The complex was synthesized by adopting a similar procedure as for **2** by using solid $NaN(CN)_2$ (0.3561 g, 5 mmol) instead of NaSCN (yield 71%). Anal. Calcd. for $C_{25}H_{30}N_8O_7Mn$ (**3**): C, 49.26; H, 4.96; N, 18.38. Found: C, 49.06; H, 4.88; N, 18.31%.

3.4. Catalytic activities and kinetic studies

The kinetics of the 3,5-DTBC and TCC oxidation was determined by the initial rates method by monitoring the increase of the product 3,5-DTBQ (at 423, 422 and 423 nm for **1**, **2**, and **3**, respectively) and of the product TCQ (at 428, 430 and 425 nm for **1**, **2** and **3**, respectively). The concentration of the substrate 3,5-DTBC and TCC was always kept at least 10 times larger than that of the Mn^{II} complex so as to maintain the pseudo-first-order condition. All of the kinetic experiments were conducted at constant temperature of 20 °C, monitored with a thermostat. Initially, a series of solutions of substrate 3,5-DTBC and TCC having different concentrations (8×10^{-4} to 5×10^{-2} mol dm^{-3}), were prepared from a substrate concentrated stock solution using methanol as solvent. Then, 2 mL of such substrate solution was poured in a 1 cm quartz cell and kept in the spectrophotometer to equilibrate the temperature at 20 °C. A 0.04 mL (2 drops) of 5×10^{-3} mol dm^{-3} of Mn^{II} complex in methanol was quickly added and mixed thoroughly to get an ultimate Mn^{II} complex concentration of 1×10^{-4} mol dm^{-3} and the absorbencies were measured accordingly. Initial rates were determined from slope of the tangent to the absorbance vs time curve at $t = 0$. By applying *GraFit32* program for enzymatic kinetics, K_m and V_{max} are calculated from the graphs, and the inset shows the Lineweaver–Burk plot. k_{cat} values were calculated by dividing the V_{max} values with the concentration of the corresponding complexes. Furthermore, for a particular substrate concentration, varying the Mn^{II} complex concentration, a linear relationship for the initial rates was obtained, which shows a first order dependence on the Mn^{II} complex concentration. On the other hand, varying the concentration of substrates 3,5-DTBC and TCC, a first-order dependence was observed at low 3,5-DTBC and TCC concentration. However, all Mn^{II} complexes showed a saturation kinetic at higher 3,5-DTBC and TCC concentrations. Thus a treatment on the basis of Michaelis–Menten model was seemed to be appropriate.

Similar procedure as described above was adopted to study phosphatase activity by using PNPP as substrate. The reactions were spectroscopically monitored by the increase of the product PNP at 436 nm for **1** and at 435 nm for **2**, while **3** forms an adduct with PNPP and therefore no kinetic study was performed for the latter.

3.5. X-ray data collection and structure determination

Diffraction data for the structures reported were collected at room temperature on a Nonius DIP-1030H system and on a BRUKER SMART APEX diffractometer (in both cases Mo Kα radiation, λ = 0.71073 Å) equipped with CCD. Cell refinement, indexing and scaling of the data sets were carried out using Bruker SMART APEX and SAINT package [39], Denzo, and Scalepack programs [40]. The crystal of **2** revealed to be weakly diffracting (θ_{max} angle 23.4°), but the results obtained are of good quality. The structures were solved by direct methods and subsequent Fourier analyses [41]

and refined by the full-matrix leastsquares method based on *F*2 with all observed reflections [41]. The crystal of complex **1** shows a disordered location of one ethylene ligand bridge (0.61/0.39 occupancy), of a nitrate anion (disordered over two positions sharing two oxygens), and of another nitrate, which is close to a centre of symmetry. Two residuals close to the disordered nitrates were interpreted as lattice water molecules (H atoms not located). All these species have a fixed occupancy of 0.5. Hydrogen atoms placed at geometrically calculated positions were included in final cycles of refinements. All the calculations were performed using the WinGX System, Ver 1.85.05 [42]. Crystallographic data for all the complexes are given in Table 3.

4. Conclusions

With the aim to synthesize dinuclear manganese(II) complexes on reaction with dinucleating compartmental ligand, L, formed by condensation between 2,6-diformyl-4-methylphenol and 2-(2-aminoethyl)pyridine we get mononuclear manganese(II) complexes instead. All the three synthesized mono-manganese(II) complexes are observed to be excellent catalysts towards the oxidation of 3,5-DTBC and TCC and the hydrolysis of PNPP (except **3** that forms an adduct). To the best of our knowledge this is the first report where Mn^{II} complexes exhibit this behavior. The catalytic efficiency of the complexes was assessed by following conventional Michaelis–Menten enzymatic kinetics. The protonation of one of the imine N atoms of ligand L, as revealed from X-ray single crystal structure analysis, is supposed to be the key factor for (i) obtaining mono-nuclear species instead of the expected dinuclear ones and (ii) the observed extraordinary catalytic activities of the three mono-manganese(II) species.

Supplementary data

IR and EPR spectra for complexes, enzyme kinetics data for complexes **2** and **3**, blank experiments with substrates TCC and PNPP. Supplementary crystallographic data are available from the Cambridge Crystallographic Data Centre, 12, Union Road, Cambridge CB2 1EZ, UK (Fax: +44 1223 336033; e-mail: deposit@ccdc.cam.ac.uk) on request, quoting deposition number 787430 and 787431.

Acknowledgements

The authors wish to thank the University Grants Commission, New Delhi [UGC Major Research Project, F. No. 34-308\2008 (SR) Dated: 31.12.2008 (DD) for financial support. A.G. is thankful to Shailabala Biswas Research Foundation, University of Calcutta for financial support.

Appendix A. Supplementary data

Supplementary data associated with this article can be found, in the online version, at doi:10.1016/j.molcata.2011.01.025.

References

[1] H. Sakiyama, H. Okawa, R. Isobe, J. Chem. Soc., Chem. Commun. (1993) 882.
[2] H. Sakiyama, H. Tamaki, M. Kodera, N. Matsumoto, H. Okawa, J. Chem. Soc., Dalton Trans. (1993) 591.
[3] H. Sakiyama, H. Okawa, M. Suzuki, J. Chem. Soc., Dalton Trans. (1993) 3832.
[4] C. Higuchi, H. Sakiyama, H. Okawa, R. Isobe, D.E. Fenton, J. Chem. Soc., Dalton Trans. (1994) 1097.
[5] A.F. Kolodziej, Prog. Inorg. Chem. 41 (1994) 493.
[6] S.J. Lippard, Science 268 (1995) 996.
[7] S. Uozumi, M. Ohba, H. Okawa, D.E. Fenton, Chem. Lett. (1997) 673.
[8] S. Uozumi, H. Furutachi, M. Ohba, M. Okawa, D.E. Fenton, K. Shindo, S. Murata, D.J. Kitko, Inorg. Chem. 37 (1998) 6281.
[9] D.E. Fenton, Chem. Soc. Rev. 28 (1999) 159.
[10] M. Suzuki, H. Furutachi, H. Okawa, Coord. Chem. Rev. 200–202 (2000) 105.
[11] P.A. Vigato, S. Tamburini, Coord. Chem. Rev. 248 (2004) 1717, and references therein.
[12] I.A. Koval, P. Gamez, C. Belle, K. Selmeczi, J. Reedijk, Chem. Soc. Rev. 35 (2006) 814, and references therein.
[13] (a) T. Chattopadhyay, M. Mukherjee, A. Mondal, P. Maiti, A. Banerjee, K.S. Banu, S. Bhattacharya, B. Roy, D.J. Chattopadhyay, T.K. Mondal, M. Nethaji, E. Zangrando, D. Das, Inorg. Chem. 49 (2010) 3121;
(b) K.S. Banu, T. Chattopadhyay, A. Banerjee, S. Bhattacharaya, E. Suresh, M. Nethaji, E. Zangrando, D. Das, Inorg. Chem. 47 (2008) 7083;
(c) A. Banerjee, S. Ganguly, T. Chattopadhyay, K.S. Banu, A. Patra, S. Bhattacharya, E. Zangrando, D. Das, Inorg. Chem. 48 (2009) 8695.
[14] J.W. Whittaker, in: A. Sigel, H. Sigel (Eds.), Metal Ions in Biological Systems, vol. 37, Marcel Dekker, New York, 2000, p. 587.
[15] L. Que Jr., M.F. Reynolds, in: A. Sigel, H. Sigel (Eds.), Metal Ions in Biological Systems, vol. 37, Marcel Dekker, New York, 2000, p. 505.
[16] H. Biava, C. Palopoli, C. Duhayon, J.P. Tuchagues, S. Signorella, Inorg. Chem. 48 (2009) 3205.
[17] A.J. Wu, J.E. Penner-Hahn, V.L. Pecoraro, Chem. Rev. 104 (2004) 903.
[18] G. Auling, H. Follmann, in: A. Sigel, H. Sigel (Eds.), Metal Ions in Biological Systems, vol. 30, Marcel Dekker, New York, 1994, p. 131.
[19] D.E. Ash, J.D. Cox, D.W. Christianson, in: A. Sigel, H. Sigel (Eds.), Metal Ions in Biological Systems, vol. 37, Marcel Dekker, New York, 2000, p. 407.
[20] A. Zouni, H.T. Witt, J. Kern, P. Fromme, N. Krauss, W. Saenger, P. Orth, Nature 409 (2001) 739.
[21] N. Kamiya, J.R. Shen, Proc. Natl. Acad. Sci. U.S.A. 100 (2003) 98.
[22] C. Tommos, G.T. Babcock, Acc. Chem. Res. 31 (1998) 18.
[23] C.F. Yocum, C.T. Yerkes, R.E. Blakenship, R.R. Sharp, G.T. Babcock, Proc. Natl. Acad. Sci. U.S.A. 78 (1981) 7507.
[24] N.A. Law, M.T. Caudle, V.L. Pecoraro, Adv. Inorg. Chem. 46 (1999) 305–440.
[25] K. Nakamoto, Infrared and Raman Spectra of Inorganic and Coordination Compounds, 3rd ed., Wiley, New York, 1978.
[26] R.H. Holm, E.I. Solomon, Guest Editors, Chem. Rev. 96 (1996) 2435.
[27] E.I. Solomon, U.M. Sundaram, T.E. Machonkin, Chem. Rev. 96 (1996) 2563.
[28] W. Kaim, J. Rall, Angew. Chem. 108 (1996) 47;
Angew. Chem., Int. Ed. Engl. 35 (1996) 43.
[29] J. Kaizer, R. Csonka, G. Barath, G. Speier, Transit. Met. Chem. 32 (2007) 1047.
[30] A. Majumder, S. Goswami, S.R. Batten, M.S. El Fallah, J. Ribas, S. Mitra, Inorg. Chim. Acta 359 (2006) 2375.
[31] F.H. Westheimer, Science 235 (1987) 1173.
[32] B.L. Vallee, D.S. Auld, Proc. Natl. Acad. Sci. U.S.A. 87 (1990) 220.
[33] P. Molenveld, J.F.J. Engbersen, D.N. Reinhoudt, Chem. Soc. Rev. 29 (2000) 75.
[34] J.A. Tainer, E.D. Getzoff, J.S. Richardson, D.C. Richardson, Nature 306 (1983) 284.
[35] J.S. Valentine, M.W. Pantoliano, in: T.G. Spiro (Ed.), Copper Proteins, Krieger Publishing Co., Malabar, FL, 1981, p. 291.
[36] J.S. Valentine, D.J. Mota de Freitas, Chem. Educ. 62 (1985) 990.
[37] J.V. Bannister, W.H. Bannister, G. Rotilio, CRC Crit. Rev. Biochem. 22 (1987) 111.
[38] R.R. Gagne, C.L. Spiro, T.J. Smith, C.A. Hamann, W.R. Thies, A.K. Shiemeke, J. Am. Chem. Soc. 103 (1981) 4073.
[39] SMART, SAINT, Software Reference Manual, Bruker AXS Inc., Madison, WI, USA, 2000.
[40] Z. Otwinowski, W. Minor, in: C.W. Carter Jr., R.M. Sweet (Eds.), Methods in Enzymology, Macromolecular Crystallography, Part A, vol. 276, Academic Press, New York, 1997, p. 307.
[41] G.M. Sheldrick, Acta Crystallogr. A64 (2008) 112.
[42] L.J. Farrugia, J. Appl. Crystallogr. 32 (1999) 837.